Non-Linear SNR Degradation of Mixed 10G/100G Transmission Over Dispersion-Managed Networks

Emanuele Virgillito[1], Stefano Straullu[2], Andrea Castoldi[3], Rosanna Pastorelli[3], Vittorio Curri[1]

[1] *DET, Politecnico di Torino, Torino, Italy, emanuele.virgillito@polito.it*
[2] *LINKS Foundation, Torino, Italy, stefano.straullu@linksfoundation.com*
[3] *SM-Optics, Vimercate, Italy, andrea.castoldi@sm-optics.com*

Abstract: Enabling the mixed 10G IMDD with 100G coherent channels transmission over legacy dispersion-managed links on metro network chunks will come in handy for the operators to increase network flexibility while saving on CAPEX and operate progressive upgrades with no impact on existing traffic. We developed a semi-analytical model for 10G-to-100G XPM noise allowing QoT estimation on mixed 10G/100G systems.

1. Introduction

Polarization-division-multiplexed (PM) coherent transmission technology delivering 100 Gbps and larger data-rates dominates the backbone network market made up of fiber links without dispersion compensation units (DCU). On the contrary, the metro and access network segment still largely employs legacy intensity modulated, direct detected (IMDD) channels delivering 10 Gbps on dispersion managed (DM) optical line systems (OLS). Although the complete migration of these systems to coherent technology is foreseen, such upgrade would require large CAPEX, making this operation not convenient until the technical development makes coherent systems cheaper. In the meantime, a realistic scenario envisages the transmission of mixed 10G and 100G optical channels on DM OLS, so that the knowledge of the propagation impairments arising in such a situation is crucial for network planning and management. A typical use-case is depicted in Fig.1(a), where some 100G channels would be routed through a section of a DM metro network, which can be already loaded with existing 10G traffic. Hence, it is fundamental to be able to predict all the impairment arising in the whole optical path in order to keep under control the quality of transmission (QoT) of the 100G channel and route it transparently through the mixed 10G/100G section.

It is known that coherent transmission undergoes intense non-linear interference (NLI) from DM OLS [1] and from IMDD channels [2, 3]. Penalties from 10G channels are traditionally mitigated by setting a guard-band between the 10G and the 100G channels combs [2], as depicted in Fig.1(b). Among the non-linear 10G-to-100G effects, the most significant one is the cross phase modulation (XPM) originated by a 10G channel on a 100G channel, which can be splitted in an additive noise contribution and a multiplicative non-linear phase noise (NLPN). In [4], we have shown that, in the worst-case scenario of polarization-aligned 10G channel to a 100G channel, the XPM manifests itself essentially as NLPN on the 100G phase in DM OLS with a small amount of residual inline chromatic dispersion D_{RES}. However, state-of-the-art coherent receivers based on digital signal processing (DSP) with Carrier Phase Estimation (CPE) are able to track and compensate for the NLPN. Hence, the remaining part of the 10G-to-100G XPM is an additive noise whose effect is managed within the generalized signal to noise ratio (GSNR) of the 100G channel, which is thus taken as the unique merit figure of the QoT [5]. Here, we assume that this noise source arises by the interaction of the XPM phase noise with polarization effects [4]. In fact, since the 10G channels are polarized, the interplay of the XPM with birefringence and PMD principal axes rotation should be considered [6]. This interaction

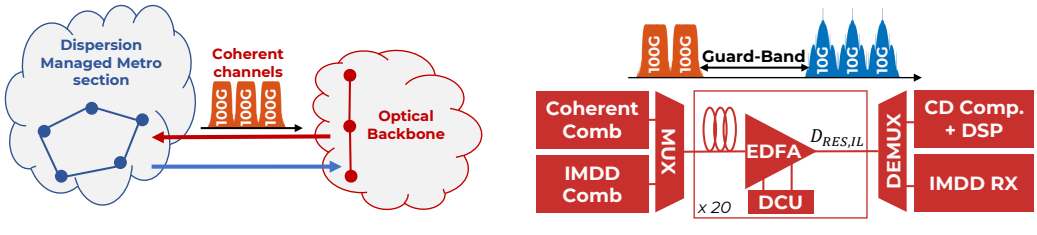

(a) (b)

Fig. 1: (a) Network routing scenario: a comb of 100G coherent channels gets routed through a section of DM metro network. (b) Scenario for mixed 10G/100G transmission over 20 span of DM OLS. The DCU leaves D_{RES} ps/nm of residual dispersion at the end of each span.

gives rise to a non-linear crosstalk (NL-XT) of one polarization state to the other, which manifests itself as an additive noise. So, three independent sources of additive noise degrade the 100G channels QoT: the amplified spontaneous emission (ASE) noise added by the optical amplifiers, the NLI generated by the 100G-to-100G interaction and the NL-XT originated by the 10G.

In this paper, we focus on the estimation of the NL-XT part. This would enable a network controller to set guard-bands between 10G and 100G and channel powers in order to keep under control the SNR degradation on the 100G channel due to the co-existence with the 10G lightpaths. Starting from the analytical model proposed in [4], in Sec. 2 we derive a simple yet effective semi-analytical expression of the NL-XT noise variance. Due to the stochastic nature of the birefringence and PMD, in Sec. 3, the model outcome has been compared to the probability density function (PDF) estimations of the GSNR obtained by running Monte-Carlo simulations on different random birefringence using Split-Step Fourier method (SSFM) simulations of the coupled non-linear Schroedinger equation [7] The model showed to scale properly with the system parameters, providing an always conservative NL-XT evaluation which comes in handy to avoid random out-of-service due to extreme realizations of the birefringence and PMD induced rotation of principal axes.

2. Analytical model

In this section we will derive a simple analytical expression estimating the SNR due to the NL-XT additive noise. As already introduced in Sec. 1, assuming that the NLPN can be completely recovered, the GSNR is the unique QoT parameter for the 100G channels which considers all the impairments in the mixed 10G-100G transmission on DM OLS. The SNR due to the single noise sources sum up in parallel, so that:

$$\frac{1}{\text{GSNR}} = \frac{1}{\text{OSNR}} + \frac{1}{\text{SNR}_{\text{NL}}} + \frac{1}{\text{SNR}_{\text{NL-XT}}} \tag{1}$$

where the OSNR takes into account the ASE noise only, the SNR_{NL} considers the NLI generation among 100G channels alone and the $\text{SNR}_{\text{NL-XT}}$ is the additive noise originated by the interaction of the 10G-to-100G XPM with the polarization effects. Here, both in the model and the simulations campaign, in order to isolate the NL-XT phenomenon, we assume that the optical amplifiers do not introduce any noise and that NLI is negligible by considering a single 100G probe channel with sufficiently low power to avoid self-channel effects. Under these assumptions, the 10G NL-XT is the unique impairment left on the 100G channel, so that $\text{GSNR} = \text{SNR}_{\text{NL-XT}}$.

A simple analytical expression for $\text{SNR}_{\text{NL-XT}}$ is derived following the approach in [4]. We assume that a 10G pump writes a pure NLPN through XPM on each of the two 100G probe polarization modes, indicated as X and Y. Then, the NLPN is transformed into an additive noise crosstalk due to the polarization modes coupling caused by birefringence. Consequently, $\vec{E}_R(t) = \bar{T}(t) \cdot \vec{E}_T(t)$, where $\vec{E}_T(t) = [E_{Tx}(t), E_{Ty}(t)]^\intercal$ and $\vec{E}_R(t) = [E_{Rx}(t), E_{Ry}(t)]^\intercal$ are the Jones vector representation of the transmitted and received 100G probe signal after N_s spans of propagation and $\bar{T}(t) = \bar{\Phi}(t) \cdot \bar{R}$ is the 2x2 OLS transmission matrix:

$$\bar{T}(t) = e^{j\bar{\phi}(t)} \begin{bmatrix} e^{j\Delta\phi(t)} & 0 \\ 0 & e^{-j\Delta\phi(t)} \end{bmatrix} \begin{bmatrix} \cos\theta e^{j\psi} & -\sin\theta e^{-j\psi} \\ \sin\theta e^{j\psi} & \cos\theta e^{-j\psi} \end{bmatrix} \tag{2}$$

As in [4], both $\bar{\phi}(t)$ and $\Delta\phi(t)$ are the stochastic processes related to the NLPN written by the 10G pump on the 100G probe X and Y polarization modes. The first is a common NLPN term to both polarizations, the second is the differential NLPN term depending on an initial relative polarization state angle between the 10G and 100G channels. When the 10G is aligned in polarization with the X or Y polarizations of the probe the NLPN differential term is maximized. The matrix R represents an equivalent polarization rotation in the Jones space due to birefringence, with $-\pi/2 < \theta < \pi/2$ and $-\pi/4 < \psi < \pi/4$. We assumed an ideal receiver estimating the time average of the transmission matrix $\langle \bar{T}(t) \rangle$, computing its inverse and applying it to the received signal $\vec{E}_R(t)$. Hence, the decision signal is $\vec{E}_{R,DSP}(t) = \bar{T}_{res}(t) \cdot \vec{E}_T(t)$, being $\bar{T}_{res}(t)$ the matrix of the residual impairment.

$$\bar{T}_{res}(t) = \langle \bar{T}(t) \rangle^{-1} \cdot \bar{T}(t) = e^{j\bar{\phi}_e(t)} \begin{bmatrix} \sin^2\theta e^{-j\Delta\phi_e(t)} + \cos^2\theta e^{j\Delta\phi_e(t)} & -j\sin 2\theta \sin\Delta\phi_e(t) e^{-j2\psi} \\ -j\sin 2\theta \sin\Delta\phi_e(t) e^{j2\psi} & \sin^2\theta e^{j\Delta\phi_e(t)} + \cos^2\theta e^{-j\Delta\phi_e(t)} \end{bmatrix} \tag{3}$$

where $\bar{\phi}_e(t) = \bar{\phi}_e(t) - \bar{\phi}_a$, $\Delta\phi_e(t) = \Delta\phi(t) - \Delta\phi_a$ are random processes of the differences between the common mode and differential phase noise terms and their averages $\bar{\phi}_a$, $\Delta\phi_a$ estimated by the DSP. The terms on the diagonal of Eq.3 relate the received polarization component with their transmitted counterpart and they are mainly responsible for phase noise. The antidiagonal terms of $\bar{T}_{res}(t)$ generate the NL-XT noise due to IMDD-induced XPM. Hence, the NL-XT

noise process is $N_{\text{NL-XTx/y}}(t) = -j\sin 2\theta \sin\Delta\phi_e(t)e^{\mp j2\psi}\cdot E_{T\text{x/y}}(t)$. The $\text{SNR}_{\text{NL-XT}}$ is obtained as the ratio between the 100G probe power $P_{ch} = E[|E_{T\text{x/y}}(t)|^2]$ and the NL-XT noise power $E[|N_{\text{NL-XTx/y}}(t)|^2]$, being $E[|\cdot|]$ the statistical expected value operator:

$$\text{SNR}_{\text{NL-XT}} = \frac{1}{\sin^2 2\theta E[|\sin\Delta\phi_e(t)|^2]} \tag{4}$$

Eq.4 provides a very simple expression for $\text{SNR}_{\text{NL-XT}}$ depending on the equivalent polarization rotation angle θ and on the variance of the differential phase noise $\Delta\phi_e(t)$ which can be evaluated with proper analytical models for XPM or from a lookup-table obtained by single polarization SSFM simulations. Fig.2 shows the estimated $\text{SNR}_{\text{NL-XT}}$ for a pump and probe configuration varying the rotation angle θ. In the considered case, the $\Delta\phi_e(t)$ has been obtained through SSFM. Pump and probe were spaced 300 GHz with launched powers -1 dBm on the pump and -20 dBm on the probe to avoid single channel NLI. Pump is 10 Gbps NRZ modulated, probe is PM-QPSK modulated with $R_s = 32$ GBaud. The fiber link was composed of 20x50 km long fiber spans with loss $\alpha = 0.18$ dB/km, chromatic dispersion $D = 12$ ps/(nm $\cdot$ km), non-linear coefficient $\gamma = 1.27$ (W $\cdot$ km)$^{-1}$. DCU perform inline dispersion undercompensation to a residual of $D_{RES} = 50$ ps/nm. The worst-case is clearly obtained for $\theta = \pi/4$ which delivers near 25.05 dB with a swing of nearly 8 dB from the best-SNR case.

3. Validation and Results

In this section we validate the semi-analytical $\text{SNR}_{\text{NL-XT}}$ estimation method with results obtained with accurate SSFM simulations. Since the 10G pumps are polarized, their interaction with the stochastic birefringence inducing PMD leads to stochastic GSNR values dependently on the particular realization of the birefringence. For full-coherent systems with only depolarized channels the non-linear propagation can be sufficiently characterized by a single GSNR value obtained solving the Manakov equation [8]. In our case-study, instead, we estimate the PDF of the GSNR by running a Monte-Carlo campaign over several realizations of the stochastic birefringence using the coupled non-linear Schroedinger equation together with the waveplate model to simulate the birefringence effects [6]. Hence, for each considered pump-probe and system configuration, the GSNR PDF determines a sufficiently accurate worst-case GSNR corresponding to a certain detrimental birefringence realization, taken as the reference value to benchmark our model. First, the model has been tested in different pump and probe configurations similar to the setup described in section 2. Tested pump-to-probe frequency guard-bands are here 100 and 200 GHz. Two dispersion values of 4 ps/(nm $\cdot$ km) and 12 ps/(nm $\cdot$ km) have been tested on two dispersion compensation schemes leaving D_{RES} of 50 ps/nm and 90 ps/nm, leading to 8 different scenarios. For each of them, the corresponding single-polarization simulation has been run to obtain the $\Delta\phi_e(t)$ statistics after $N_s = 20$ spans. The Monte-Carlo campaign has been done with 100 realizations for each scenario. Low probe power and ideal amplification ensures that the GSNR = $\text{SNR}_{\text{NL-XT}}$. The 10G pump has always been launched aligned to the X-polarization component of the 100G probe. Comparison between the estimated PDF and model to its worst case value with $\theta = \pi/4$ are reported in Fig.3. Orange vertical lines represent the model $\text{SNR}_{\text{NL-XT}}$ predictions which are largely conservative with respect to the worst-case Monte-Carlo values by roughly 6/7 dB. However, this gap remains almost the same for almost all the configurations, showing that it scales properly with the system parameters and always more conservatively with guard-band. The explanation of this gap is attributed to the hugely pessimistic hypothesis of the model which assumes the same worst-case polarization alignment at each fiber span. In particular, the slightly larger gap at broader spacings can be explained with the stronger non-linearities averaging on the two polarization modes operated by PMD [4, 6]. An heuristic rigid shift of the predicted value by 5 dB is plotted in purple. It keeps the model conservative but with a smaller gap to the Monte-Carlo results.

As final results, in Fig.4 we compare the model to Monte-Carlo SSFM simulations with a single 100G probe and 5x10G pumps. System scenario is the same of Fig.3 except for dispersion $D = 8$ ps/(nm $\cdot$ km) and 16.7 ps/(nm $\cdot$ km).

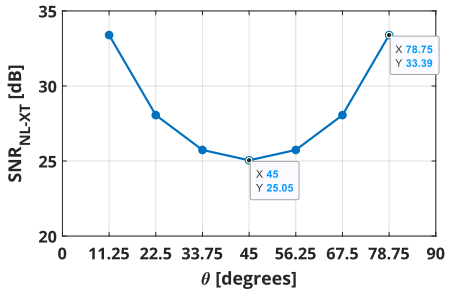

Fig. 2: $\text{SNR}_{\text{NL-XT}}$ estimation obtained with Eq.4 vs the equivalent polarization rotation angle θ

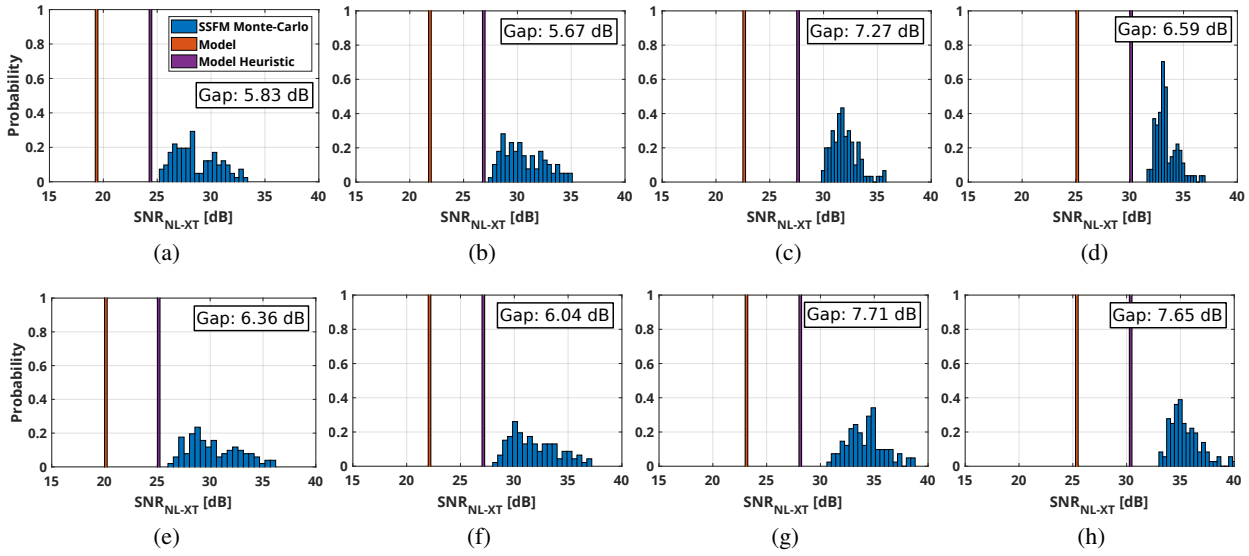

Fig. 3: Model vs SSFM pump and probe Monte-Carlo simulations: $D = 4$ (upper row), 12 ps/(nm · km) (lower row). $D_{RES} = 50$ (a,b,e,f), 90 ps/(nm · km) (c,d,g,h). Frequency spacing: 100 GHz (a,c,e,g), 200 GHz (b,d,f,h)

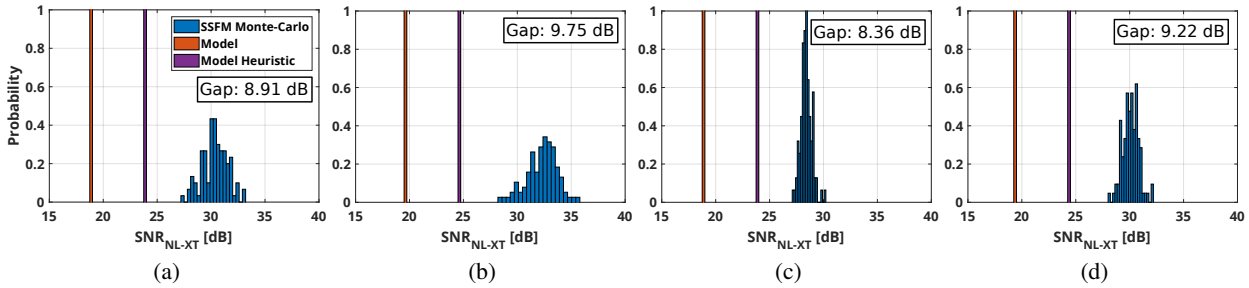

Fig. 4: Model vs 5x10G pumps SSFM Monte-Carlo simulation: $D_{RES} = 50$ ps/nm, Guard-band 300 GHz with $D = 8$ (a), 16.7 ps/(nm · km) (b). $D_{RES} = 90$ ps/nm, Guard-band 150 GHz with $D = 8$ (c), 16.7 ps/(nm · km) (d).

Also, the 10G comb to 100G probe guard-band is set to 300 GHz and 150 GHz for $D_{RES} = 50$ ps/nm and 90 ps/nm, respectively. The model prediction is obtained by calculating the single pumps $\mathrm{SNR_{NL\text{-}XT}}$ contributions and summing them up in their inverse to obtain the multi-pump model estimation; basically assuming that their noise contributions are independent. Fig.4 shows that the model is still largely conservative, with a slightly larger gap of roughly 8/9 dB with respect to SSFM worst case. This proves that the pump noise additivity holds and that the simple proposed model scales down correctly with the system parameters as seen for pump and probe case. Also, the heuristic rigid shift on the model prediction still keeps the model on the conservative side, allowing to work with smaller system margins.

4. Conclusions

We have proposed a simple and useful model to estimate the additional SNR degradation experienced by a 100G channel passing through a section of DM OLS together with legacy IMDD 10G channels. This tool can be integrated in network controllers allowing to set channel powers and/or a proper guard-band between the 10G and the 100G to control the QoT of a 100G lightpath routed through a mixed 10G/100G DM OLS. Further evolution would include the totally-analytical estimation of the $\Delta\phi_e(t)$ intensity, the abstraction of the $\mathrm{SNR_{NL\text{-}XT}}$ degradation introduced by a single span and the improvement of the estimation accuracy.

References

[1] V. Curri et al., "Dispersion Compensation and Mitigation of...", *PTL* 20.17 (2008), pp. 1473–1475.

[2] A. Carena et al., "Guard-band for 111 Gbit/s coherent PM-QPSK...", *OFC*, 2009, OThR7.

[3] J. Renaudier et al., "Investigation on WDM Nonlinear Impairments Arising...", *PTL* 21.24 (2009), pp. 1816–1818.

[4] E. Virgillito et al., "Propagation Effects...", *ICTON*, 2019, We.D1.5.

[5] M. Filer et al., "Multi-vendor experimental...", *JLT* (2018).

[6] D. Marcuse et al., "Application of the Manakov-PMD...", *JLT* 15.9 (1997), pp. 1735–1746.

[7] D. Pilori et al., "FFSS: The fast...", *ICTON 2017*, 2017, We.B1.5.

[8] M. Cantono et al., "Observing the Interaction of PMD ...", *OFC*, 2018, W1G.4.